Chemical Engineering Journal 148 (2009) 270–278

Contents lists available at ScienceDirect

Chemical Engineering Journal

journal homepage: www.elsevier.com/locate/cej

Gas–solid carbonation kinetics of Air Pollution Control residues for CO_2 storage

Valentina Prigiobbe[a], Alessandra Polettini[b], Renato Baciocchi[c,*]

[a] Institute of Process Engineering ETH Zurich, Zurich, Switzerland
[b] University of Rome "La Sapienza", Department of Hydraulics, Transportation and Roads, Rome, Italy
[c] University of Rome "Tor Vergata", Department of Civil Engineering, Via del Politecnico, Rome I-00133, Italy

ARTICLE INFO

Article history:
Received 27 March 2008
Received in revised form 22 August 2008
Accepted 25 August 2008

Keywords:
APC residues
Gas–solid mineral carbonation
CO_2 storage

ABSTRACT

Gas–solid carbonation of Air Pollution Control (APC) residues is a CO_2 Capture and Storage (CCS) technology, where highly reactive Mg- or Ca-bearing materials adsorb CO_2 and form stable Mg- or Ca-carbonates. The carbonation kinetics of this reaction have been studied at different temperatures, CO_2 concentrations, and at atmospheric pressure in order to select the best operative conditions on the basis of CO_2 stored and reaction time. The samples were initially heated up to the operative conditions under argon atmosphere and then carbonated under a CO_2–argon atmosphere. All carbonation kinetics were characterized by a rapid chemically controlled reaction followed by a slower product layer diffusion-controlled process. Maximum conversions between 60% and 80% were achieved, depending on the operative temperature and CO_2 concentration. Temperature did not notably affect the maximum conversion obtained in the experiments performed at temperatures equal or above 400 °C; the influence on the kinetics was masked by the change in initial composition due to dehydroxylation reaction and surface area while heating up to the operative temperature. A slight influence of CO_2 concentration on the kinetics was observed, whereas no influence on the maximum conversion was noticed. The obtained results suggest that the flue gases with 10 vol.% CO_2 concentration can be directly used to form stable carbonates, thus lumping capture and storage in a single step. The APC residues produced from the existing incineration plants would cover only 0.02–0.05% of the total CO_2 European storage capacity required to comply with the Kyoto protocol objectives. Nevertheless, the proposed carbonation route could be applied to other residues, such as Cement Kiln Dust, Paper mill residues and Stainless Steel Desulphurization slags, characterized by a high content of free calcium oxides and hydroxides, thus increasing the impact of this process option.

1. Introduction

Anthropogenic emissions of carbon dioxide are considered the main cause of climate change [1]. The last IPCC report [2] carries that emissions of CO_2 and other Greenhouse gases (GHGs) have increased by approximately 70% since 1970. This has prompted an increase in CO_2 concentration of almost 100 ppm in comparison to its pre-industrial level of 280 ppm [1]. Given that, prompt action in order to reverse this trend should be taken in the next decades, in particular stabilizing the GHGs concentrations in the atmosphere, e.g. CO_2. The main human activity producing CO_2 is fossil fuels combustion for energy supply, which is projected to be the dominant one until 2030 with a 40–110% CO_2 emission increase [2]. Reduction in CO_2 emissions by fossil fuels requires the implementation of Carbon Capture and Storage (CCS) systems. These first concentrate (capture) CO_2 from diluted sources to a rather pure CO_2 stream, which is then conveyed to storage. The most accredited CO_2 storage options rely on in-situ technologies, which consist in injecting CO_2 into deep saline aquifers, coal bed seams (enhanced coal bed methane recovery), oil reservoirs (enhanced oil recovery), and potentially into deep oceans (ocean storage) [1]. Although a few pilot-scale in-situ storage facilities are running, still many doubts are raised on how to assess the fate of CO_2 after injection reliably, and to avoid leakage back to the atmosphere. An alternative to the in-situ CO_2 storage approach consists in an ex-situ process based on the chemical reaction with alkaline materials bearing either calcium or magnesium. This process, known as mineral carbonation, mimics natural weathering, where CO_2 reacts exothermically with alkaline elements present in natural metal-oxide bearing material, forming thermodynamically stable and benign carbonates. Seifritz [3] proposed it for the first time, and since then several authors, e.g. [4–9], have been studying the slurry system using natural silicates such as olivine, serpentine, and wollastonite. Residues from different industrial activities have been proposed because they are a valuable source of alkalinity for the carbonation process: pulverized fuel ash produced by coal fired power stations, ground-granulated

* Corresponding author. Tel.: +39 06 72597022; fax: +39 06 72597021.
E-mail address: baciocchi@ing.uniroma2.it (R. Baciocchi).

1385-8947/$ – see front matter © 2008 Elsevier B.V. All rights reserved.
doi:10.1016/j.cej.2008.08.031

blast furnace and stainless steel slags from the steel manufacturing industry, bottom and fly municipal solid waste incineration ashes, as well as deinking ash, resulting from the waste produced during the recycling of paper [10]. These materials contain alkaline elements in a more readily available form, so that carbonation could in principle take place at less severe operative conditions than the ones needed for silicate minerals. The amount of available alkaline residues is of a scale which will allow to store only a few hundreds $ktCO_2/y$, i.e orders of magnitude below the current CO_2 emissions (25 $GtCO_2/y$). Nevertheless, the process can substantially reduce the CO_2 emissions of specific industrial sectors (e.g. cement or steel industry) and can be a way to introduce the carbonation technology [1]. Moreover, carbonation might improve the environmental behavior of the residues allowing either for their reuse or make their disposal less expensive [11]. In particular, carbonation of alkaline residues can be performed by two different reaction routes: a dry and a wet gas–solid route [11].

In the dry gas–solid carbonation route, the alkaline solid is contacted with a gas containing CO_2 at atmospheric pressure and high temperatures. Gas–solid carbonation of pure calcium and magnesium oxides has been studied theoretically by Bhatia and Perlmutter and Butt et al. [12,13]. Bhatia and Perlmutter [12] investigated the kinetics of CaO carbonation by modified TGA experiments performed in a CO_2 stream at different operative temperatures, obtaining 70% calcium conversion at 500 °C, but a still reasonably fast process rate and high carbonation efficiency when operative at 400 °C. Butt et al. [13] studied the gas–solid kinetics of $Mg(OH)_2$ carbonation. Under helium–CO_2 atmosphere in isothermal TGA experiments, they observed that dehydroxylation of brucite and precipitation of magnesite occurred simultaneously with the fastest kinetics at 375 °C.

More recently, Abanades and Alvarez [14] proposed the use of CaO in a fluidized bed to capture CO_2 directly from combustion gases. Up to 70% carbonation conversion was obtained for the fresh material, but a reduction in conversion yield was observed after several carbonation–calcination cycles, required to recover the raw material from the process. The results obtained from direct gas–solid carbonation of natural alkaline oxides, such as MgO and CaO, provide the basis for applying this route to the carbonation of alkaline residues, since such materials are largely composed of calcium and magnesium oxides or hydroxides. Nikulshina et al. [15] investigated CaO and $Ca(OH)_2$ carbonation, observing that the addition of water vapor significantly enhances the reaction kinetics to the extent that, in the first 20 min, the reaction proceeds at a rate that is 22 and 9 times faster than that observed for the dry carbonation of CaO and $Ca(OH)_2$. The first study dealing with direct gas/solid carbonation of alkaline residues was by Jia and Anthony [16], who performed pressurized TGA experiments of hydrated and non-hydrated fluidized bed combustion ash, achieving CaO conversion efficiencies up to 60% when operative at temperatures above 400 °C and in a 100% CO_2 atmosphere. Nevertheless, in this work neither further independent evidence of the degree of carbonation was provided, nor was any information given on the effect of the carbonation reaction on leaching behavior of metals. More recently, Baciocchi et al. [17] have investigated in detail the gas–solid carbonation of APC (Air Pollution Control) residues collected from an hospital wastes incinerator. Carbonation experiments were performed under 100 vol.% CO_2 atmosphere at atmospheric pressure and temperatures ranging between 300 and 500 °C. Carbonation was observed to be effective above 400 °C, with a maximum Ca conversion of 60%. Neither evidence of the temperature effect on the reaction rate was provided nor the effect of CO_2 concentration was addressed. Both these issues are investigated in this paper, with the aim of assessing the feasibility of APC residues gas–solid carbonation for a possible industrial application. In this view, the kinetics of the carbonation process is of paramount importance in order to design a proper gas–solid contacting system, which should guarantee an as low as possible residence time. Besides, the possibility of performing carbonation using flue gases rather than pure CO_2 as a reactant is also worth investigating, since this would allow to lump capture and storage in a single step. To this aim, carbonation kinetics studies of APC residues were performed in a TGA furnace under constant temperatures varying from 300 up to 500 °C and in atmosphere of CO_2-argon mixture of 10, 22, and 50 vol.% of CO_2. No water vapor was added to the gas mixture, in order to simplify the experimental procedure since in previous papers by Nikulshina et al. [15], water vapor was observed to positively affect the carbonation kinetics, the results obtained in this paper provide a conservative estimate of carbonation using flue gases,where typically water vapor is also present. This range was selected based on previous studies of our group [17], where carbonation was observed to be effective only above 300 °C, whereas starting at 600 °C $CaCO_3$ decomposition may take place. The material was characterized applying chemical elemental analysis, thermogravimetric analysis and X-ray diffraction, in order to quantify both the total calcium content and the corresponding calcium phases in the material before the carbonation experiments. The study of the chemical reaction pathways was also investigated and supported by SEM, X-ray diffraction analysis, thermogravimetric analysis, surface area and porosity measurement of untreated and treated APC residues.

2. Analytical methods

2.1. Materials and methods

APC residues were sampled at a hospital waste incinerator, located in the vicinity of Rome, from the bag-house section located downstream of a contact reactor for acid gases and organic micropollutants abatement, where $Ca(OH)_2$ and activated carbon are used as reactants. When the APC residues were received at the laboratory, they were homogenized using a quartering procedure, oven-dried at 60 °C to constant weight, and finally transferred into sealed containers, where they were kept until the time of testing to prevent contact with atmospheric CO_2.

The characterization of the APC residues, whose detailed description is reported elsewhere [18], is summarized in Table 1. The other main species include NaCl (approximately 9.5% wt.) and KCl (approximately 1.0% wt.). Their grain size ranged between 10 and 40 μm while their mineralogy, obtained by X-ray diffraction, is characterized by the presence of: CaOHCl, $Ca(OH)_2$, $CaCO_3$, $CaSO_4$, NaCl, and KCl. Among them, only CaOHCl and $Ca(OH)_2$ can undergo a carbonation reaction. CaOHCl amount was calculated assuming that Cl was distributed among the three phases NaCl, KCl and CaOHCl, while $Ca(OH)_2$ content was calculated from the TGA analysis of

Table 1
Mass fraction (x, %) of the main species in the untreated fly ash and measurement methods [18]

Species	x (%)	Measurement/assumption
$Ca(OH)_2$	37.8	Indirect calculation based on the difference between TG/DTA and calcimetry analysis and CaOHCl content
CaOHCl	28.9	Indirect calculation based on Na^+, K^+ leaching values from EN12457-2 test, Cl^- content and XRD analysis
$CaCO_3$	18.0	TG/DTA and calcimetry analysis
$CaSO_4$	4.8	Direct calculation based on SO_4^{2-} content and XRD analysis

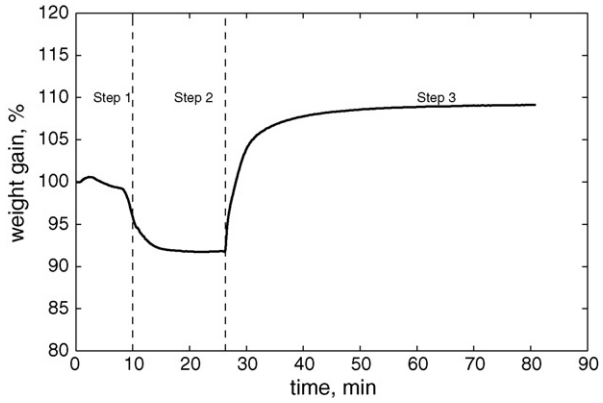

Fig. 1. Typical weight variation [%] vs. time observed during carbonation experiments.

dry fly ash once the amounts of H_2O, carbon content, CaOHCl and $CaCO_3$ were determined.

2.1.1. X-ray diffraction

XRD analyses were carried out by means of XPERT-PRO (PANALYTICAL), equipped with a copper anode (Cu Kα; λ = 1.54056 Å). The equipment's operational conditions were 40 kV, 50 mA. The 2θ range between 5° and 109° was scanned at the rate of 0.2° min^{-1}. The database from the software TOPAS 2.0 produced by Bruker was used for the identification of the crystalline phases.

2.1.2. Surface area

BET measurements of dehydrated APC residue samples were carried out by means of Micrometrics Tristar 3000 in N_2 atmosphere. The samples were heated up to the applied operative temperatures (i.e., after steps 1 and 2 of the experimental procedure, shown in Fig. 1 and described in Section 2.2) and then analyzed. The method and the interpretation of the data were implemented according to Sing et al. [19]. The results, reported in Table 2, showed that the specific surface area decreased with increasing temperature.

2.1.3. Porosity

The porosity and the pore size distribution were measured by mercury intrusion porosimetry using Micrometrics Autopore 9220 with the software Autopore II 9220 v2.03. This technique can be applied over a capillary range between 0.003 and 360 μm. Porosity measurements allowed identifying a change of the pore structure between the original sample, characterized by microporous structure (<14 μm) and the pre-heated samples (at the end of step 2), which were probably characterized by a meso-porous structure (2–50 nm). Given the analytical method applied, the data obtained at different pre-heating temperatures did not allow assessing the effect of pre-heating temperature on the pore structure. On the contrary, BET surface area was observed to decrease with increasing pre-heating temperature. This behavior might be explained by a change of the pore structure towards the formation of larger pores with increasing pre-heating temperature or might suggest the occurrence of collapse of a fraction of the original pores.

Table 2
Specific surface area of APC residues heated up to the applied operative temperatures.

Heating temperature (°C)	BET ($m^2\ g^{-1}$)
350	33.35 ± 0.61
400	29.01 ± 0.49
450	20.12 ± 0.42
500	15.90 ± 0.23

2.1.4. Scanning electron microscopy (SEM)

The morphologies of the APC residues were observed under a scanning electron microscope using Leo 1530 microscope (Zeiss/LEO, Oberkochen, Germany).

2.2. Carbonation kinetics experiments

Carbonation experiments were carried out in a thermogravimetric system (TGA, Netzsch STA 409 CD) coupled with Gas Chromatography (GC, 2-channel Varian Micro GC, equipped with a Molsieve-5A and a Poraplot-U columns) for measurement of the evolving CO_2. An average amount of 44 mg of APC residues was placed on an holder in a uniform layer of 3 mm and carbonated at different temperatures (300, 350, 400, 450, 500 °C), at a total pressure of 1 bar, and under different CO_2 concentrations obtained by mixing CO_2 (99.99% purity) with argon, as reported below:

- 10 vol.% of CO_2 and 90 vol.% of argon and total flow rate 160.5 mL min^{-1};
- 22 vol.% of CO_2 and 78 vol.% of argon and total flow rate 184.5 mL min^{-1};
- 50 vol.% of CO_2 and 50 vol.% of argon and total flow rate 239 mL min^{-1}.

Table 3 reports the operative conditions of the experimental runs, together with the main results, which are discussed in Section 3. It is worth pointing out that tests performed at the same CO_2 partial pressure, but at different temperature, actually correspond to slightly different CO_2 concentration. Nevertheless, the difference in concentration is rather small: at 10% CO_2, it ranges from 1.95 10^{-3} mol L^{-1} at 350 °C to 1.5 10^{-3} mol L^{-1} at 500 °C, at 22% CO_2, it ranges from 4.3 10^{-3} mol L^{-1} at 350 °C to 3.5 10^{-3} mol L^{-1} at 500 °C, at 50% CO_2, it ranges from 9.8 10^{-3} mol L^{-1} at 350 °C to 7.9 10^{-3} mol L^{-1} at 500 °C. For the sake of simplicity, and without any loss of generality, in the following, we will discuss all the exper-

Table 3
Experimental conditions of the carbonation experiments. $t_{50\%}$ corresponds to the time needed to achieve 50% Ca conversion.

Exp. no.	T (°C)	CO_2 (vol.%)	Final conversion (%)	$t_{50\%}$(s)
5	350	10	60.1	122
6	350	10	62.2	121
8	350	22	53.8	68
9	350	50	61.7	32
10	350	50	56.3	35
11	400	10	73.4	103
13	400	22	68.2	66
14	400	50	69.9	31
15	450	10	78.9	233
16	450	10	74.1	223
17	450	22	71.4	105
18	450	22	67.9	158
19	450	50	68.4	43
20	450	50	66.5	64
21	500	10	76.3	176
22	500	10	75.3	143
23	500	22	77.8	79
24	500	22	69.3	61
25	500	50	69.6	43

iments performed at constant CO_2 concentration as if they were performed also at constant CO_2 partial pressure. Before starting the experiment, the furnace was flushed with argon in order to achieve three volumes exchanges.

Fig. 1 reports the weight variation observed during a typical carbonation experiment, showing clearly the three steps of the experimental procedure:

- ***Step 1*: heating**. TGA furnace heated up to the desired operative temperature with a heating rate of 20 K min^{-1} and under argon flow; the weight loss observed during this step can be attributed mostly to the moisture and bond-water loss.
- ***Step 2*: idle**. TGA furnace kept at the operative temperature for 15 min again under argon flow.
- ***Step 3*: carbonation**. A constant flow of the argon–CO_2 mixture was applied while keeping T constant until the carbonation completed (2 h).

After 2 h at constant temperature and argon–CO_2 flow, the CO_2 flow was switched off and the system was cooled down to room temperature keeping only argon flowing through the furnace chamber. The sample weight and CO_2 concentration in the off-gas line were measured over time during all the experiment using TGA and GC, respectively. The final solid product was analyzed with X-ray

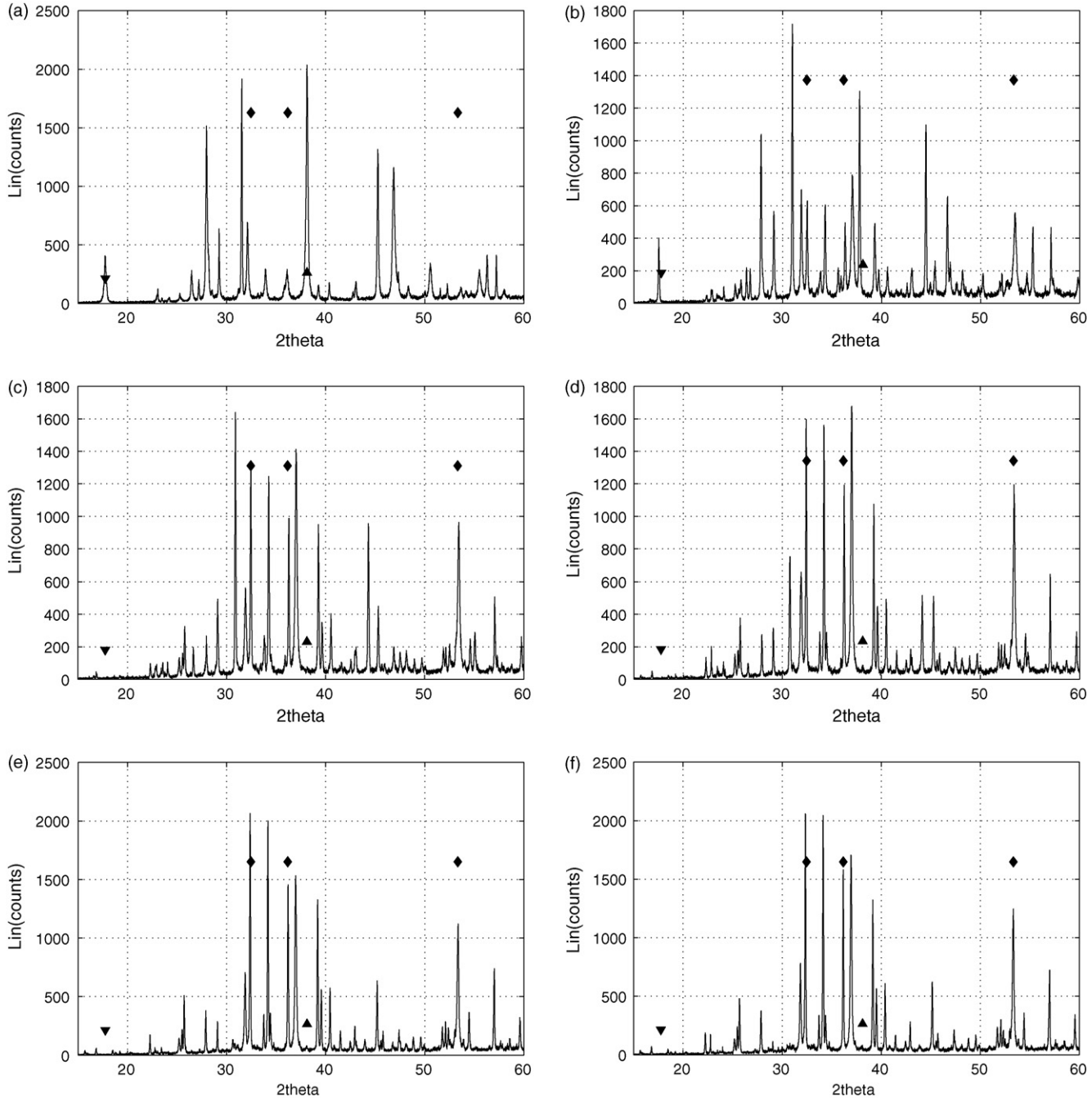

Fig. 2. X-ray patterns of APC residues performed in helium atmosphere at: (a) ambient temperature, (b) 300 °C, (c) 350 °C, (d) 400 °C, (e) 450 °C, and (f) 500 °C. Diamond symbols indicate CaO characteristic peak positions; upwards triangles indicate CaOHCl phase; and downwards triangles indicate $Ca(OH)_2$ phase.

diffraction methods to assess the formation of $CaCO_3$ at the end of each experiment.

3. Results and discussion

3.1. Identification of reactants and reaction pathways

As shown in Fig. 1, a weight decrease of the APC residue was typically observed at the end of step 1 and further also through step 2. This decrease was ascribed either to moisture loss or to the transformation of the existing phase, with water loss. Based on this evidence, and on the nature of the compounds present in the residues, it was supposed that the reacting phases available at the beginning of the carbonation experiments could be different from those present in the original material, depending on the operative temperature. X-ray diffraction analysis, SEM images and TGA measurements of the untreated material have been used as analytical techniques to identify the reactive phases at the applied operative temperatures and to describe the reaction pathways.

The identification of the reacting species by performing XRD analysis of pre-heated samples was carried out at different temperatures under helium atmosphere, i.e. 25, 300, 350, 400, 450, and 500 °C. From the patterns shown in Fig. 2, it can be noticed that the characteristic peaks of $Ca(OH)_2$ and CaOHCl are still present in the sample pre-heated at 300 °C, suggesting that the mineralogy of the samples was substantially unchanged with respect to the as-received material, at least as far as $Ca(OH)_2$ and CaOHCl are concerned. On the contrary, XRD patterns of all the other samples, pre-heated at a temperature equal or higher than 350 °C, showed the peaks of CaO; whereas those corresponding to $Ca(OH)_2$ and CaOHCl were not detected. However, $Ca(OH)_2$ and CaOHCl could still be present in the material, but as amorphous phases that cannot be observed with X-ray analysis.

The results of TGA of untreated APC ash under argon atmosphere at 20 K min^{-1} from 25 to 1000 °C reported in Fig. 3 clearly show two main weight changes. The first one took place between 300 and 500 °C, and it can be attributed to the dehydroxylation of both $Ca(OH)_2$ and CaOHCl to CaO in agreement with the findings of Allal et al. [20]. The second one, between 500 and 700 °C is linked to $CaCO_3$ decomposition and confirmed the results already obtained in a previous paper [17]. The total weight loss observed up to 700 °C is equal to about 21%, it is very close to the stoichiometric weight loss expected from the dehydroxylation of $Ca(OH)_2$ and CaOHCl (reactions (1) and (2)), equal to 12%, and from the $CaCO_3$ decomposition, equal to 8%, (reaction (5)). The difference between the expected value from the dehydroxylation (12%) and the measured one (8%) suggests that a fraction of undecomposed hydroxides might still be present at 500 °C.

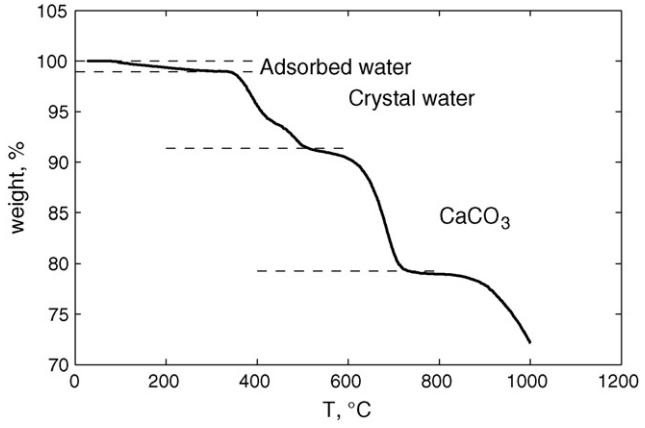

Fig. 3. TGA thermogram of a sample of untreated APC residue.

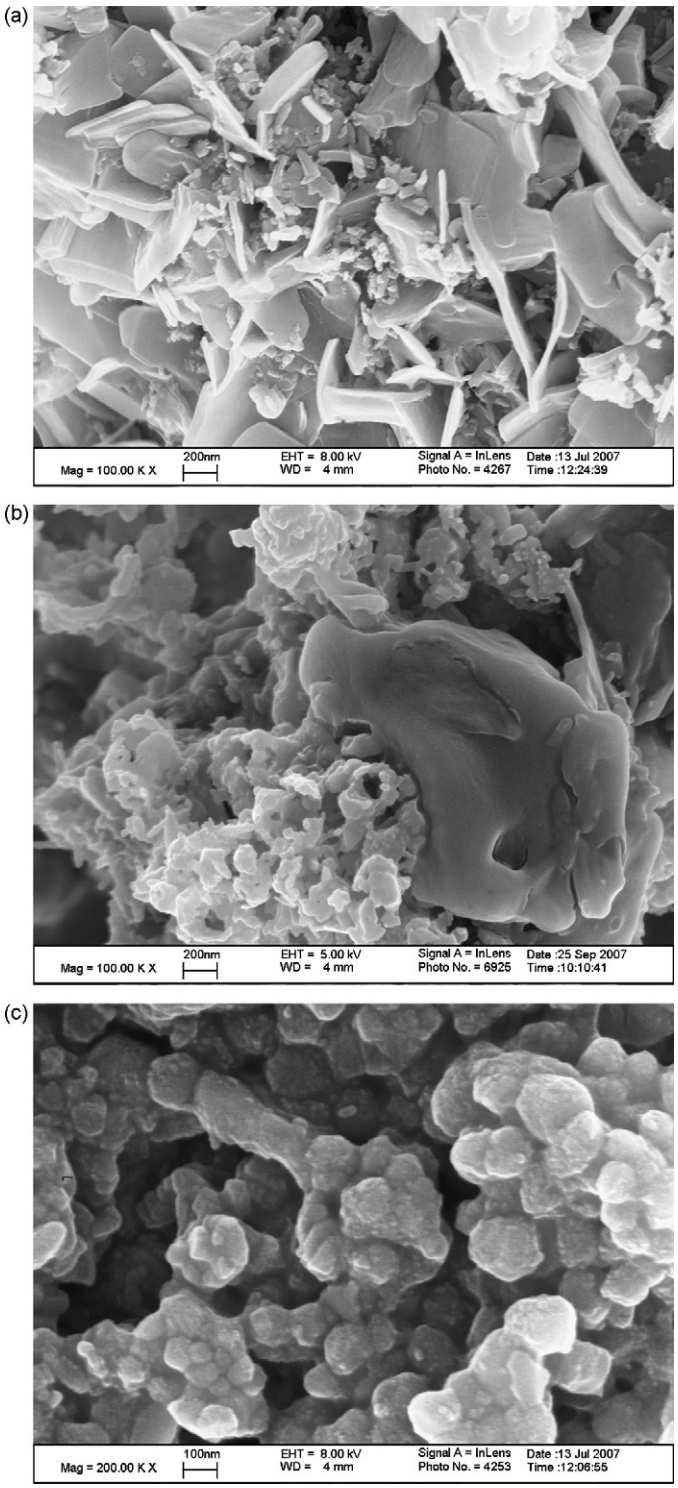

Fig. 4. SEM pictures of APC residues before and after the carbonation experiment 10 at 350 °C and applying 50 vol.% of CO_2. (a) Untreated sample; (b) dehydrated sample, at the end of step 2; (c) carbonated sample, at the end of step 3.

Fig. 4 reports the SEM images of APC samples. These measurements have been carried out in order to characterize the reacting phases by the morphology of the samples. They correspond to the three experimental steps described in Section 2.2 during run 10,

performed at 350 °C. A visual analysis of these images leads to the following observations:

- The morphology of the untreated sample, shown in Fig. 4(a), is layer-like which is the characteristic shape of CaOHCl and $Ca(OH)_2$.
- After dehydroxylation (step 2), shown in Fig. 4(b), some crystals were observed, which could be attributed to CaO, characterized by an iso-rhombic–hexagonal morphology. Nevertheless, the layer-like morphology of $Ca(OH)_2$ and CaOHCl is still evident. This suggests that the sample still contains unreacted CaOHCl and $Ca(OH)_2$ at this temperature but part of the CaOHCl might have already been transformed into CaO.
- After the carbonation reaction (step 3) sample particles, shown in Fig. 4(c), are more rounded and the layer-like structure disappeared completely. Such a variation can be attributed to the formation of $CaCO_3$, whose typical crystal shape is trigonal–hexagonal–scalenohedral.

The evidence gained from the different qualitative analysis suggests that $Ca(OH)_2$ and CaOHCl were only partially converted to calcium oxide, so that all three calcium species were present at the different operative temperatures, before the onset of the carbonation reaction. The amount of the calcium species available at the different operative temperature was estimated from the weight loss data measured in each experiment during steps 1 and 2. In doing this, the following assumptions were made:

- The weight loss at the end of step 2 was assumed to be only due to the release of water from the following decomposition reactions [20]:

$$2CaOHCl_{(s)} \rightarrow CaCl_{2(s)} + CaO_{(s)} + H_2O_{(g)} \quad (1)$$

$$Ca(OH)_{2(s)} \rightarrow CaO_{(s)} + H_2O_{(g)} \quad (2)$$

- Reactions (1) and (2) were supposed to occur in parallel and at the same rate. This assumption may not correspond to physics, but is considered reasonable for the scope of this work.

Using these assumptions, the actual fraction of water loss was calculated as the ratio between the weight loss measured at the end of step 2 and the theoretical total water released as if CaOHCl and $Ca(OH)_2$ were dehydroxylated completely. These values are shown in Fig. 5 for each applied temperature. The average water loss measured at 300 °C was negligible in comparison to the total water content bound to $Ca(OH)_2$ and CaOHCl whereas it increased for temperatures from 300 to 400 °C, and stabilized at temperatures higher than 450 °C. Given the assumption discussed above, the percentage of water loss with respect to the stoichiometric value was used to estimate through reactions (1) and (2) the percentage of $Ca(OH)_2$ and CaOHCl converted to CaO.

From these data, it was also straightforward to characterize quantitatively the composition of the sample at the beginning of step 3, in terms of CaOHCl, $Ca(OH)_2$, and CaO content, the latter one also reported in Fig. 5.

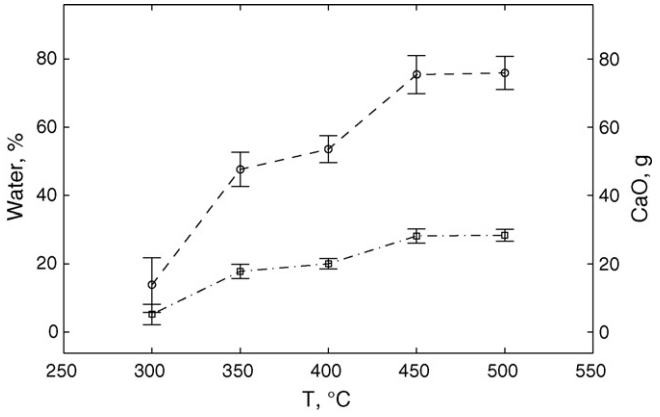

Fig. 5. Water weight loss (○) and mass of CaO (□) formed from $Ca(OH)_2$ and CaOHCl dehydroxylation for 100 g of untreated APC residues at different applied operating temperatures. The lines are only a visual guide.

3.2. Estimation of carbonation conversion

The thermogravimetry data corresponding to the carbonation reaction (step 3 in Fig. 1) were analyzed assuming that all the three calcium species available could react with CO_2 simultaneously through the following gas–solid exothermic reactions:

$$CaOH_{2(s)} + CO_{2(g)} \rightarrow CaCO_{3(s)} + H_2O_{(g)} \quad (3)$$

$$2CaOHCl_{(s)} + CO_{2(g)} \rightarrow CaCO_{3(s)} + CaCl_{2(s)} + H_2O_{(g)} \quad (4)$$

$$CaO_{(s)} + CO_{2(g)} \rightarrow CaCO_{3(s)} \quad (5)$$

The conversion of the carbonation reaction was evaluated as the ratio between the measured weight increase, $\delta W(t)$ [g], and the maximum weight increase expected from the complete carbonation of the reacting phases, i.e. $Ca(OH)_2$, CaOHCl, and CaO, δW^{conv}_{stoic} [g], calculated as follows.

$$\delta W^{conv}_{stoic} = n_{Ca(OH)_2}(\omega - \theta) + \frac{n_{CaOHCl}(\omega - \theta)}{2} + n_{CaO}\omega \quad (6)$$

where ω and θ are the molecular weights of CO_2 and water, respectively; $n_{Ca(OH)_2}$, n_{CaOHCl}, and n_{CaO} correspond to the moles of $Ca(OH)_2$, CaOHCl, and CaO, respectively, at the beginning of step 3. This equation clearly shows that the weight change is due to the uptake of CO_2, but also due to the water loss because of the dehydroxylation of $Ca(OH)_2$ and CaOHCl. This needs to be accounted for in order to evaluate the extent of the carbonation reaction, $\eta^{conv}(t)$, correctly, which is given by:

$$\eta^{conv}(t) = \frac{\delta W(t)}{\delta W^{conv}_{stoic}} 100 \quad (7)$$

The conversion measured at the end of step 3, which represents the maximum conversion of the carbonation reaction for each run, is reported for the different applied operative conditions in Table 3. The complete data of the carbonation kinetics in terms of conversion vs. time are reported in Figs. 6 and 7.

3.3. Results of carbonation kinetics

Most of the kinetics of carbonation, reported in Fig. 6, showed a similar shape, characterized by a first induction period corresponding to $CaCO_3$ nucleation, followed by a rapid growth reaction and by a slower final reaction stage at higher conversions. As suggested by Bhatia and Perlmutter [12] for CaO carbonation, the initial rapid growth step increase can be assumed to be kinetically controlled by the carbonation reactions (reactions (3–5)) during which $CaCO_3$ crystals form a layer gradually reducing the porosity of the sample. This behavior is consistent with the observation that the residues are characterized by large pores (mesoporous structure), which exclude diffusion-controlled kinetics. After a given reaction time, the product layer hinders further diffusion of CO_2 into the material, switching the process to a diffusion-controlled one.

Looking at the results reported in Fig. 6, it can be noticed that at 350 °C the final Ca conversion values varied between 54% and 62%, and no trend could be recognized among the runs carried out at different CO_2 concentrations.

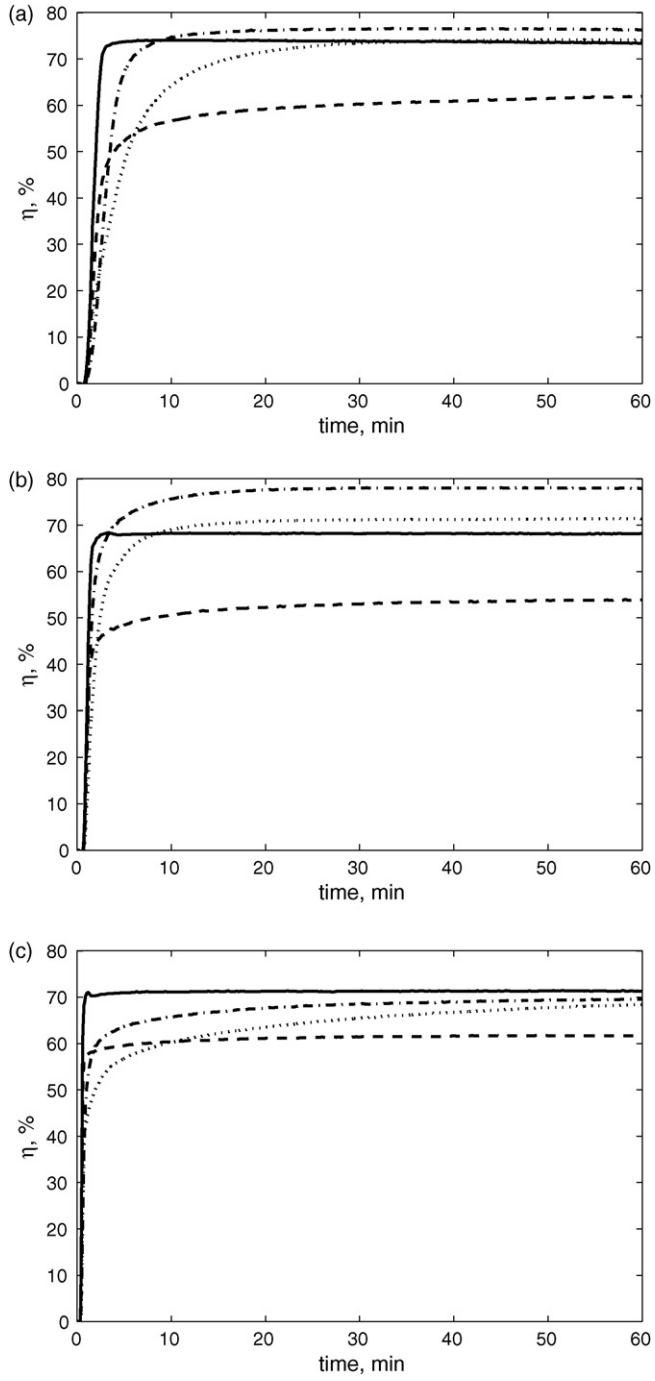

Fig. 6. Calcium conversion vs. time: (a) 10 vol.% of CO_2; (b) 22 vol.% of CO_2; (c) 50 vol.% of CO_2 at different temperatures: 350 °C (- - -) runs 5, 8, and 9; 400 °C (—) runs 11, 13, and 14; 450 °C (···) runs 15, 17, and 19; 500 °C (-·-·-) runs 21, 23, and 25.

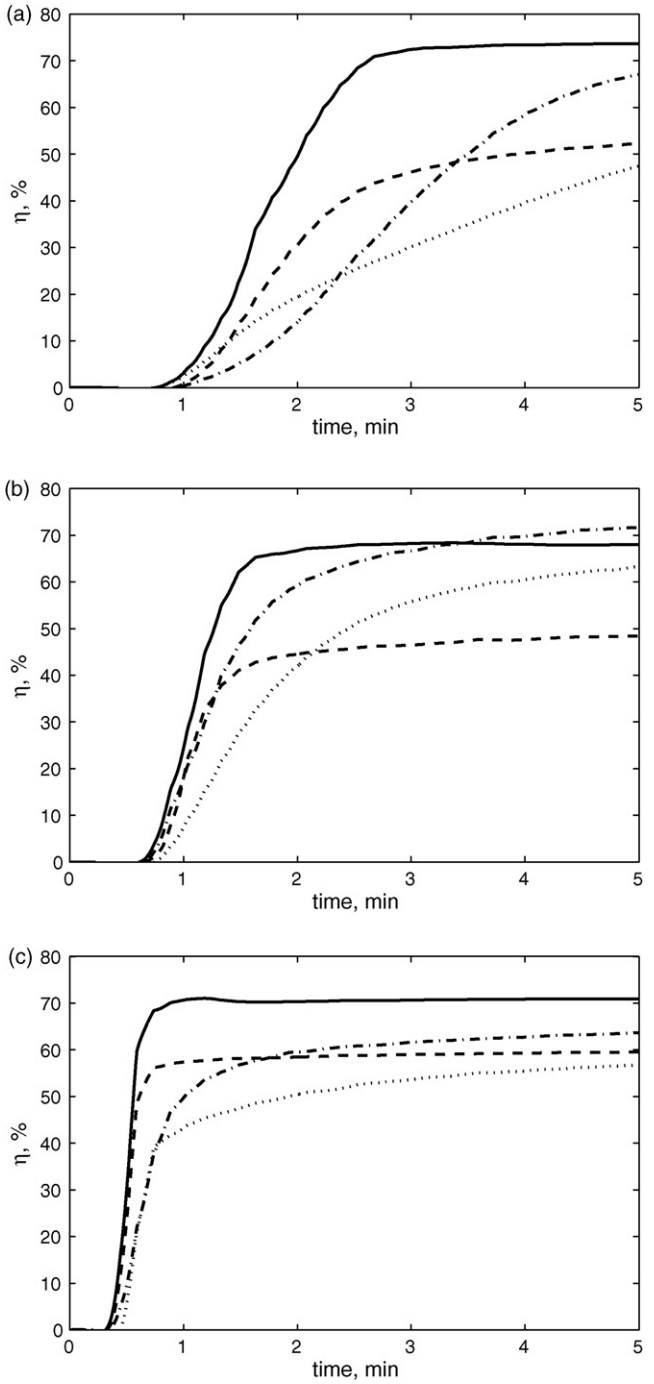

Fig. 7. Calcium conversion vs. time in the first 5 min: (a) 10 vol.% of CO_2; (b) 22 vol.% of CO_2; (c) 50 vol.% of CO_2 at different temperatures: 350 °C (- - -) runs 5, 8, and 9; 400 °C (—) runs 11, 13, and 14; 450 °C (···) runs 15, 17, and 19; 500 °C (-·-·-) runs 21, 23, and 25.

The experiments performed at 400 °C (11, 13, and 14) showed a different characteristic shape of calcium conversion vs. time curves. Conversion was observed to increase very rapidly, reaching in few minutes approximately the maximum value, and to remain almost constant until the end of the run. Such a discontinuity in the reaction rate could be attributed to the particular physical changes of the particles, i.e. a sudden decrease in porosity, tortuosity and total pore size due to $CaCO_3$ precipitation, agglomeration of particles, sintering, etc. occurring only at this temperature value. During run 14 characterized by the fastest observed kinetics the curve reached a maximum value and then slightly decreased until a stable one. This behavior might be due to a buoyancy effect which takes place at the very beginning of step 3 when the total gas flux fed to the TGA furnace is suddenly increased since CO_2 is added to the Ar flow. For this reason, such an effect could be appreciated only in the experiment characterized by the fastest kinetics and not in the other ones. Also at this temperature calcium conversion, shown in Table 3, was not much affected by the applied CO_2 concentrations although the highest calcium conversion was measured at 10 vol.% CO_2 concentration (run 11).

At 450 °C, the shape of the kinetics curves was characterized by a smooth change between the chemically-controlled phase and the diffusion-limited one, as observed in the experiments performed at 350 °C. The values of maximum conversion achieved were higher than at 400 °C varying between 68% and 73%, with the highest value achieved in runs at 10 vol.% of CO_2 (15 and 16), while the conversion decreased as the applied CO_2 concentration increased.

Finally, at 500 °C, the highest maximum extent of reaction was achieved although the carbonation kinetics was not the fastest one. That could be due to a faster $CaCO_3$ precipitation in the material pore that soon further hindered CO_2 diffusion into the material. Summarizing the main experimental evidence, it can be concluded that the operative temperature did not greatly affect the final maximum conversion of the reaction, despite the decrease of the material surface area with increasing temperature (see Table 2). The only exception was represented by the experiments performed at 350 °C, where the maximum reaction conversion was lower than the one measured under other operative conditions. On the contrary, experiments at the same operative temperature but at different CO_2 concentrations did not show any special trend, although the highest conversion was obtained at 10 vol.% CO_2. This is an encouraging result, in the perspective of applying carbonation directly to the flue gases of a combustion plant whose composition is typically around 10 vol.% CO_2, thus opening the possibility of lumping both CO_2 capture and storage in a single process.

Finally, a deeper insight into the carbonation reaction was obtained by looking at the detail of the kinetics in the very first minutes of the reaction (Fig. 7), and considering the $t_{50\%}$ values in Table 3 which correspond to the time required to achieve 50% of the final Ca conversion. Looking at Fig. 7, it is evident that CO_2 concentration has an important effect on the first stage of the carbonation kinetics. The slope of the chemically-controlled stage, during which the conversion increases rapidly and almost linearly with time, was observed to increase with increasing CO_2 concentration. This different behavior is also reflected in increasing values of the time required to achieve 50% of the maximum conversion, $t_{50\%}$, reported in Table 3. On the other hand, the effect of temperature cannot be clearly assessed from the trend of both $t_{50\%}$ and $\eta^{conv}(t)$ during the first 5 min. That could be due to two main phenomena occurring during the experiments:

(1) the composition of the material changed as the operative temperature changed, as highlighted above;
(2) the specific surface area, reported in Table 2, decreased as the operative temperature changed.

Nevertheless, it is worth pointing out that the lowest $t_{50\%}$ values were observed in the experiments performed at 400 °C, which was always characterized by the steepest conversion curve in the chemically-controlled stage. In view of a full scale application, a short residence time would be desired in order to reduce the reactor size. Therefore, the operative condition of $T = 400$ °C and CO_2 concentration 50 vol.%, where 1 min is needed to achieve the maximum conversion, should be selected. However, this would require to capture CO_2 previously from the flue gases, where the typical CO_2 concentration is around 10 vol.% An alternative approach would consist in performing the process at the same temperature but at 10 vol.% CO_2 concentration, which, despite requiring a longer residence time (i.e., 2.5 min), would allow to lump capture and storage in a single step since flue gases could be directly used as the gas feed. It is worth pointing out that in real combustion flue gases, the presence of water vapor is actually expected to speed up the carbonation kinetics [15], thus further reducing the required residence time.

4. Conclusion

Mineral carbonation is a CCS technology where CO_2 reacts with natural silicate and industrial alkaline materials and forms stable carbonate. Although the latter are available in smaller amount than the former, the use of industrial alkaline materials is attracting since they are very reactive and, most of the time, available at the CO_2 production. In this paper, we have reported the study of gas–solid carbonation of a type of alkaline material, APC residues. A fundamental study based on XRD, TGA and SEM analysis allowed to evaluate the composition of the APC residues after pre-heating under inert atmosphere and just before carbonation started. It was shown that, by increasing the pre-heating temperature, the weight fraction of $Ca(OH)_2$ and CaOHCl originally present in the material is reduced, whereas the CaO one is increased. In this way, the raw isothermal TGA data (weight vs. time), measured in a TGA furnace under a CO_2/Ar flux, could be transformed in terms of calcium conversion vs. time at different operating conditions. The results of carbonation kinetics, shown and discussed in this paper, confirmed that the carbonation process is effective at temperatures equal to or above 350 °C. Maximum conversions between 60% and 80% were obtained, depending on the operative temperature and CO_2 concentration. The kinetics were characterized by a rapid chemically-controlled reaction followed by a slower product layer diffusion-controlled process. Apart from the tests performed at 350 °C, the influence of temperature on the maximum conversion was negligible. Besides, the influence of temperature on the rate of the carbonation reaction was masked by the different composition and surface area of the residues at the tested operative temperatures. Kinetics was slightly affected by CO_2 concentration, although the fastest kinetics was observed at 400 °C and 50 vol.% CO_2. Reasonably fast reaction rates were observed at 10 vol.% CO_2 concentration. The data collected in this paper show for the first time that carbonation of APC residues, i.e. an alkaline residue rich of free calcium oxides and hydroxides, can be carbonated under a gas stream whose composition closely resembles that of combustion flue gases. The latter would also contain water vapor, but it is likely that this would actually speed up rather than slow down the carbonation kinetics. This makes possible lumping the capture and storage processes in a single step by directly contacting the flue gases with the residues. The required operative condition can be reasonably found along the flue gas pathway of any combustion plant, making the implementation of the process feasible. The APC residues produced from the existing incineration plants would cover only 0.02–0.05% of the total CO_2 European storage capacity required to comply with the Kyoto protocol objectives. Nevertheless, the proposed carbonation route could be applied to other residues, such as Cement Kiln Dust, Paper mill residues and Stainless Steel Desulphurization slags, characterized by a high content of free calcium oxides and hydroxides, thus increasing the impact of this process option.

Acknowledgements

The authors wish to acknowledge Prof. Dr. Aldo Steinfeld, Viktoriya von Zedtwitz-Nikulshyna and Elena Galvez for the TGA and BET measurements, and Carlo Bernasconi for the XRD measurements.

References

[1] IPCC, Special Report on Carbon Dioxide Capture and Storage, Cambridge University Press, Cambridge, 2005.
[2] IPCC, Fourth Assessment Report, Mitigation of Climate Change, Cambridge University Press, Cambridge, 2007.
[3] W. Seifritz, CO_2 disposal by means of silicates, Nature 345 (1990) 486–1486.

[4] K.S. Lackner, C.H. Wendt, D.P. Butt, E.L. Joyce, D.H. Sharp, Carbon-dioxide disposal in carbonate minerals, Energy 20 (1995) 1153–1170.
[5] A.-H.A. Park, R. Jadhav, L.S. Fan, CO_2 mineral sequestration: chemically enhanced aqueous carbonation of serpentine, CJChE 81 (2003) 885–890.
[6] A.-H.A. Park, L.S. Fan, CO_2 mineral sequestration: physically activated dissolution of serpentine and pH swing process, Chem. Eng. Sci. 59 (2004) 5241–5247.
[7] G.H. Wolf, G. Chizmeshya, J. Diefenbacher, A. McKelvy, In situ observation of CO_2 sequestration reactions using a novel microreaction system, Environ. Sci. Technol. 38 (2004) 932–936.
[8] H. Béarat, M.J. Mckelvy, A.V.G. Chizmeshya, D. Gormley, R. Nunez, R.W. Carpenter, K. Squires, G.H. Wolf, Carbon sequestration via aqueous olivine mineral carbonation: role of passivating layer formation, Environ. Sci. Technol. 40 (2006) 4802–4808.
[9] S.J. Gerdemann, W.K. O'Connor, D.C. Dahlin, L.R.M. Penner, H. Rush, Ex situ aqueous mineral carbonation, Environ. Sci. Technol. 41 (2007) 2587–2593.
[10] D.C. Johnson, A solution for carbon dioxide overload, SCI Lect. Pap. Ser. 108 (2000) 1–10.
[11] G. Costa, R. Baciocchi, A. Polettini, R. Pomi, C.D. Hills, P.J. Carey, Current status and perspectives of accelerated carbonation processes on municipal waste combustion residues, Environ. Monit. Assess. 135 (2007) 55–75.
[12] S.K. Bhatia, D.D. Perlmutter, Effect of the product layer on the kinetics of the CO_2-lime reaction, AIChE J. 29 (1983) 79–86.
[13] D.P. Butt, K.S. Lackner, C.H. Wendt, S.D. Conzone, H. Kung, Y.-C. Lu, J.J. Bremser, Kinetics of thermal dehydroxylation and carbonation of magnesium hydroxide, J. Am. Ceram. Soc. 79 (1996), 1982-1898.
[14] J.C. Abanades, D. Alvarez, Conversion limits in the reaction of CO_2 with lime, Energy Fuels 17 (2003) 308–315.
[15] V. Nikulshina, E. Galvez, A. Steinfeld, Kinetic analysis of the carbonation reactions for the capture of CO_2 from air via the $Ca(OH)_2$–$CaCO_3$–CaO solar thermochemical cycle, Chem. Eng. J. 129 (2007) 75–83.
[16] L. Jia, E.J. Anthony, Pacification of FBC ash in a pressurized TGA, Fuel 79 (2000) 1109–1114.
[17] R. Baciocchi, A. Polettini, R. Pomi, V. Prigiobbe, V. Nikulshina, A. Steinfeld, CO_2 Sequestration by direct gas–solid carbonation of air pollution control (APC) residues, Energy Fuels 20 (2006) 1933–1940.
[18] R. Baciocchi, G. Costa, A. Polettini, R. Pomi, E. Di Bartolomeo, E. Traversa, Leaching Behaviour and CO_2 Sequestration Capacity of Accelerated Carbonated MSWI APC Residues, in: Proceedings of the 11th International Waste Management and Landfill Symposium, Sardinia, CIPA Publisher, Cagliari, 2007.
[19] K.S.W. Sing, D.H. Everett, R.A.W. Haul, L. Moscou, R.A. Pierotti, J. Rouquerol, T. Siemieniewska, Reporting physisorption data for gas/solid systems—with special reference to the determination of surface area and porosity, Pure & Appl. Chem. 57 (1985) 603–619.
[20] K.M. Allal, J.C. Dolignier, G. Martin, Determination of thermodynamical data of calcium hydroxichloride, Revue De L'istitut Francais du Pétrole 32 (1997) 361–368.